

Electronic Supporting Information

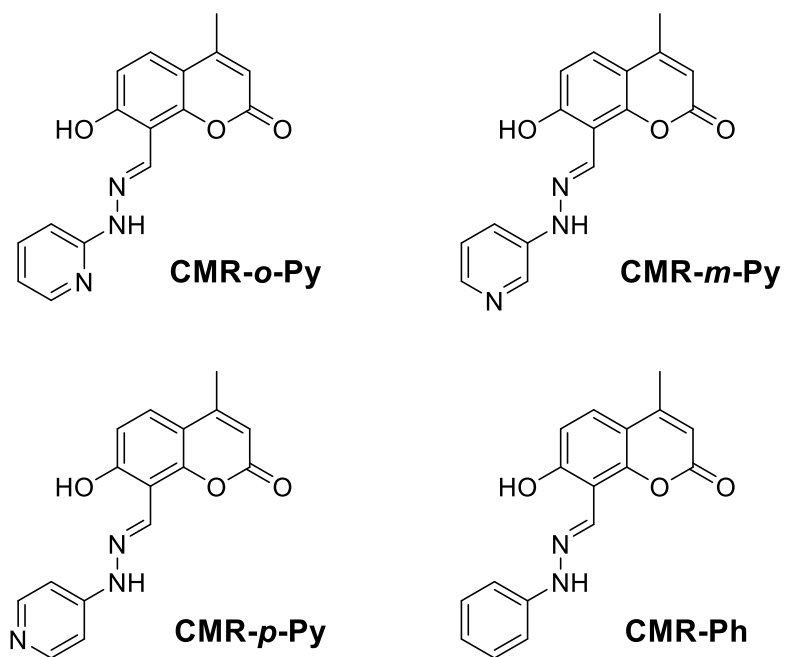
**Structural isomerism engineering regulates molecular AIE
behavior and application in visualizing endogenous hydrogen
sulfide**

Yaxi Li^{a,1}, Yong-Xiang Wang^{b,1}, Dujuan Liu^a, Chen-Chieh Ni^b,
Jianming Ni,^a and Jen-Shyang Ni^{b,*}

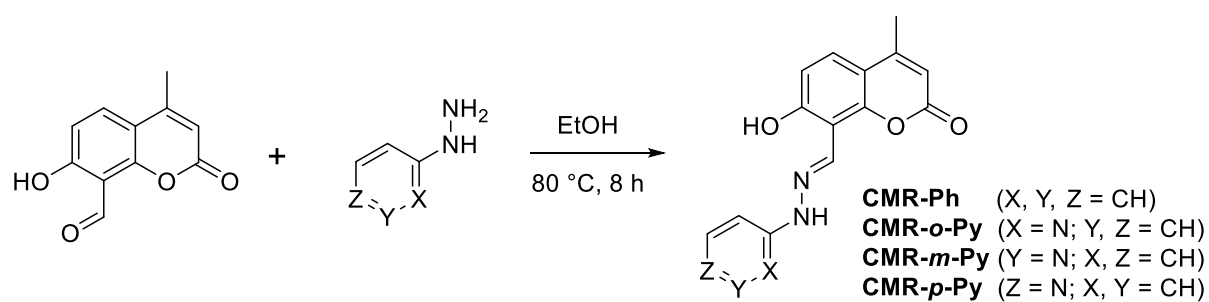
^a *Department of Radiology, Jiangnan University Medical Center (JUMC), Wuxi
214002, China*

^b *Department of Chemical and Materials Engineering, Photo-sensitive Material
Advanced Research and Technology Center (Photo-SMART), National
Kaohsiung University of Science and Technology, Kaohsiung 80778, Taiwan*

¹ *These authors contributed equally to this work.*



Scheme S1. The chemical structures of coumarin-based materials.



Scheme S2. The synthesis route of coumarin-based materials.

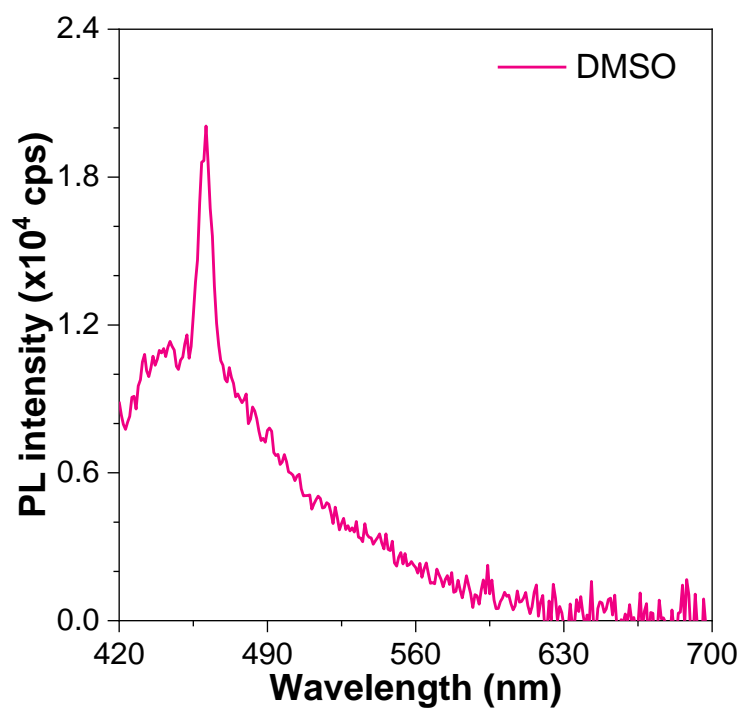


Figure S1. The PL spectra of DMSO solvent. Excitation wavelength: 400 nm; Slit: 5 nm.

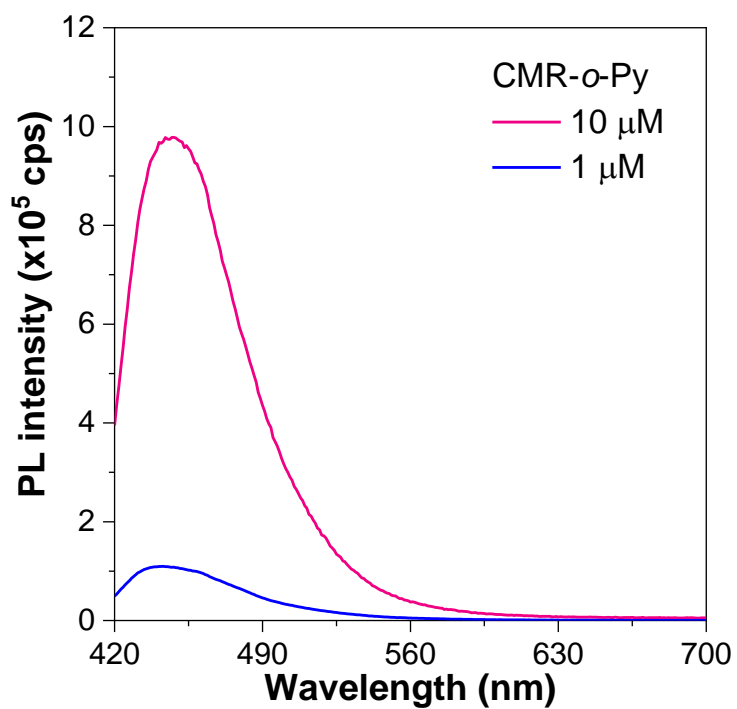


Figure S2. The PL spectra of CMR-*o*-Py in DMSO at the concentrations of 1 and 10 μM, respectively. Excitation wavelength: 400 nm; Slit: 5 nm.

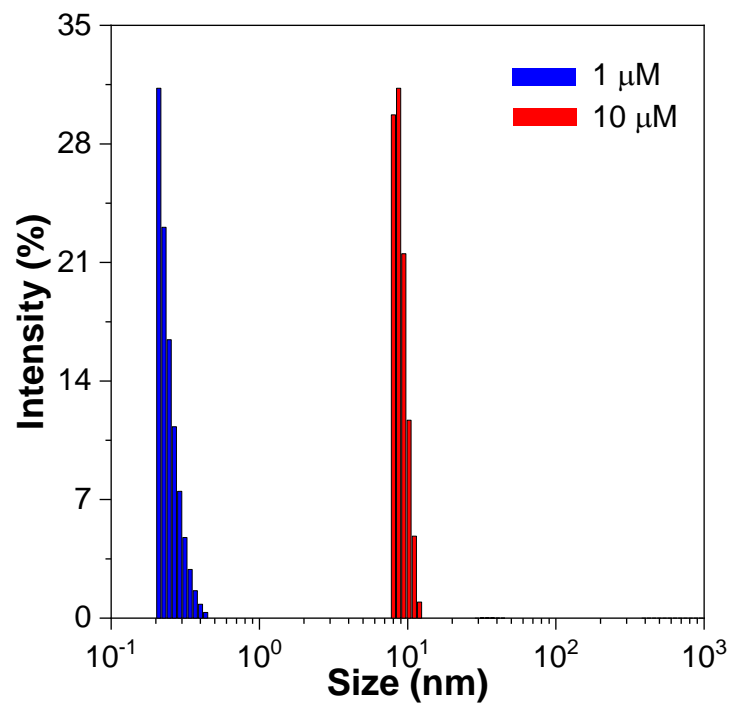


Figure S3. The DLS spectra of CMR-*o*-Py in DMSO at the concentrations of 1 and 10 μM , respectively.

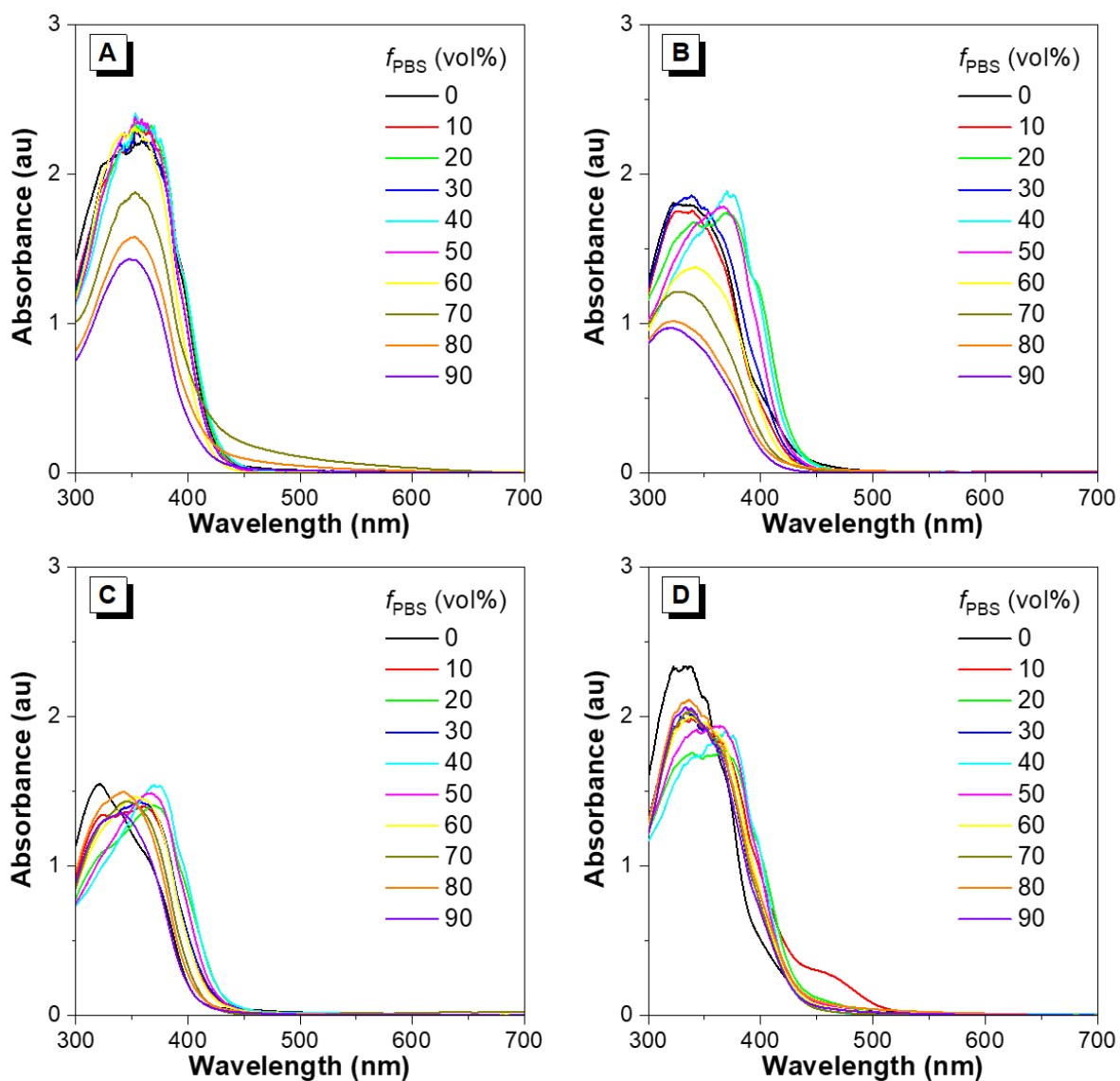


Figure S4. UV-vis absorption spectra of (A) CMR-Ph, (B) CMR-*o*-Py, (C) CMR-*m*-Py, and (D) CMR-*p*-Py in DMSO/PBS mixture solution (100 μM) with different PBS fractions (f_{PBS}).

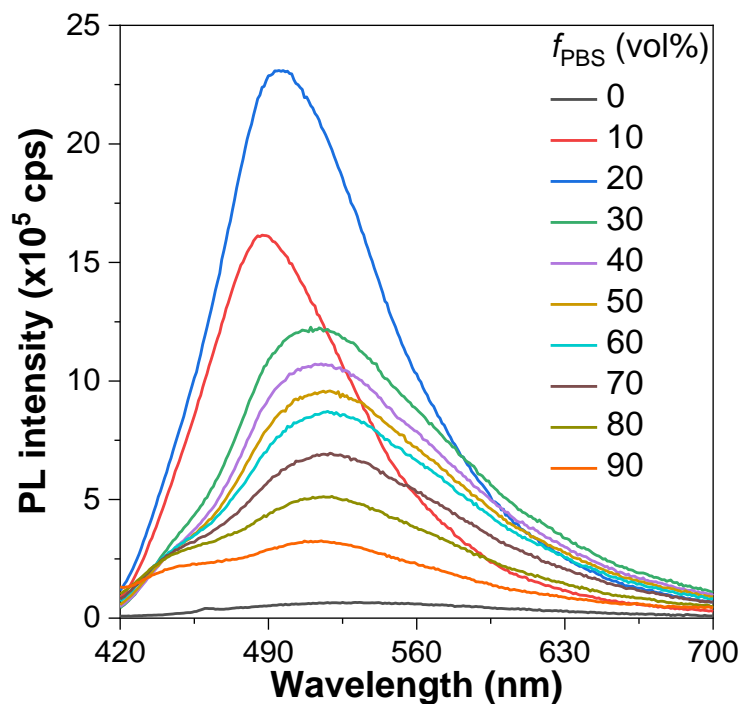


Figure S5. PL spectra of CMR-*m*-Py in DMSO/PBS mixture solution with different PBS fractions (f_{PBS}) at a concentration of 100 μM . Excitation wavelength: 405 nm; excitation slit: 1 nm; emission slit: 5 nm.

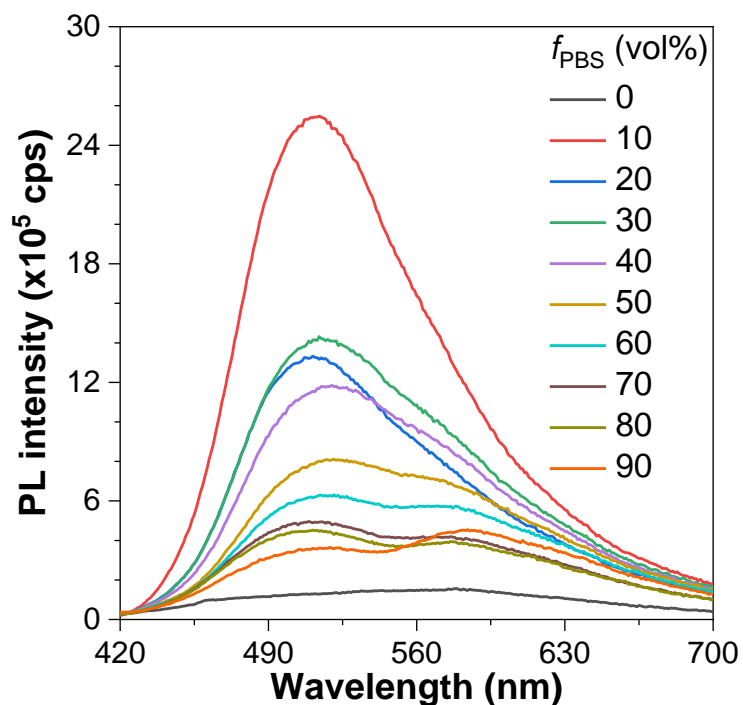


Figure S6. PL spectra of CMR-*p*-Py in DMSO/PBS mixture solution with different f_{PBS} (100 μM). Excitation wavelength: 405 nm; excitation slit: 1 nm; emission slit: 5 nm.

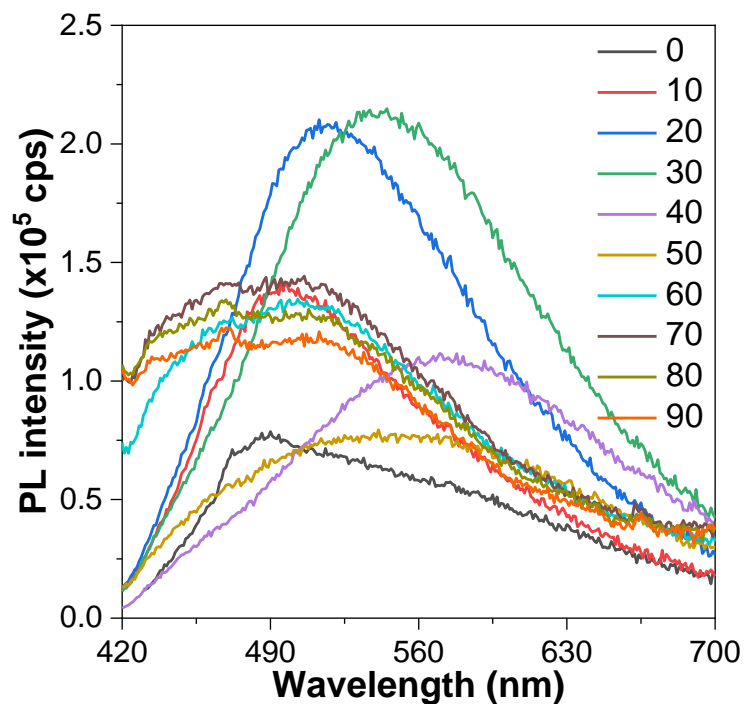


Figure S7. PL spectra of CMR-Ph in DMSO/PBS mixture solution with different f_{PBS} (100 μM). Excitation wavelength: 405 nm; excitation slit: 1 nm; emission slit: 5 nm.

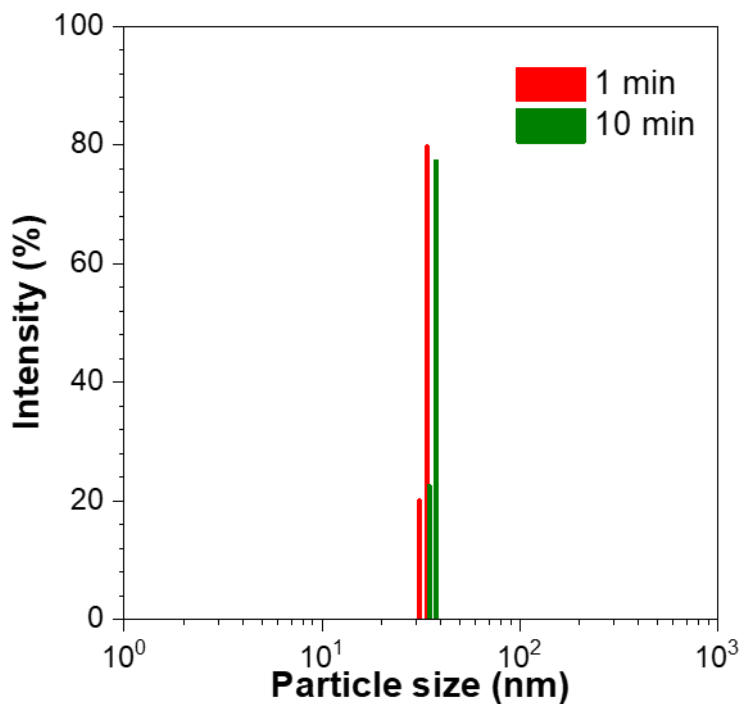


Figure S8. The DLS analysis of CMR-o-Py nanoaggregates in 90 vol% PBS solution (100 μM) after 1 and 10 min sitting, respectively.

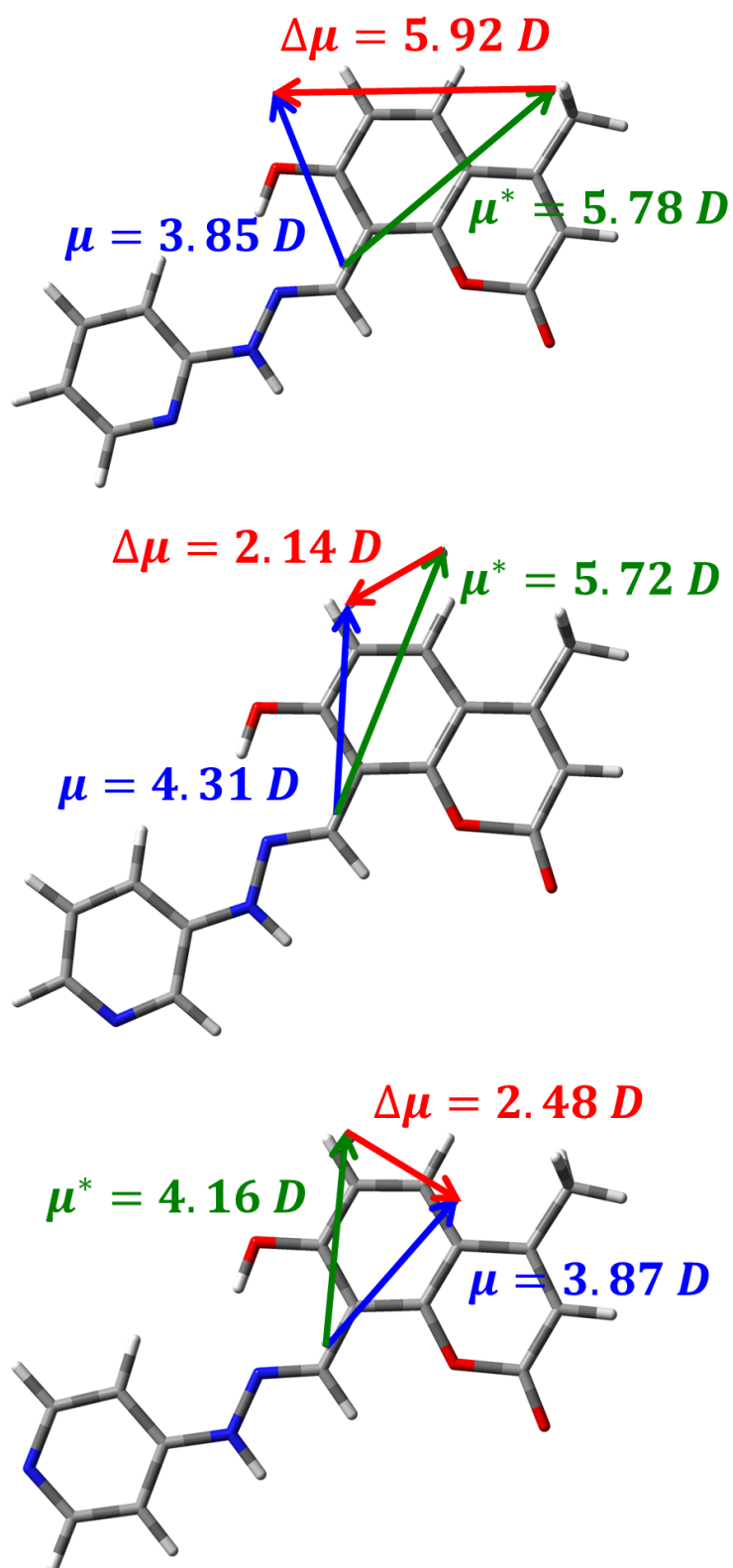


Figure S9. The dipole moment of CMR-*o*-Py, CMR-*m*-Py, and CMR-*p*-Py, respectively, calculated with TD-DFT using B3LYP functional with a 6-31G(d) basis set. μ and μ^* are dipole moments of the ground and excited states, respectively. $\Delta\mu$ is the difference value between μ and μ^* .

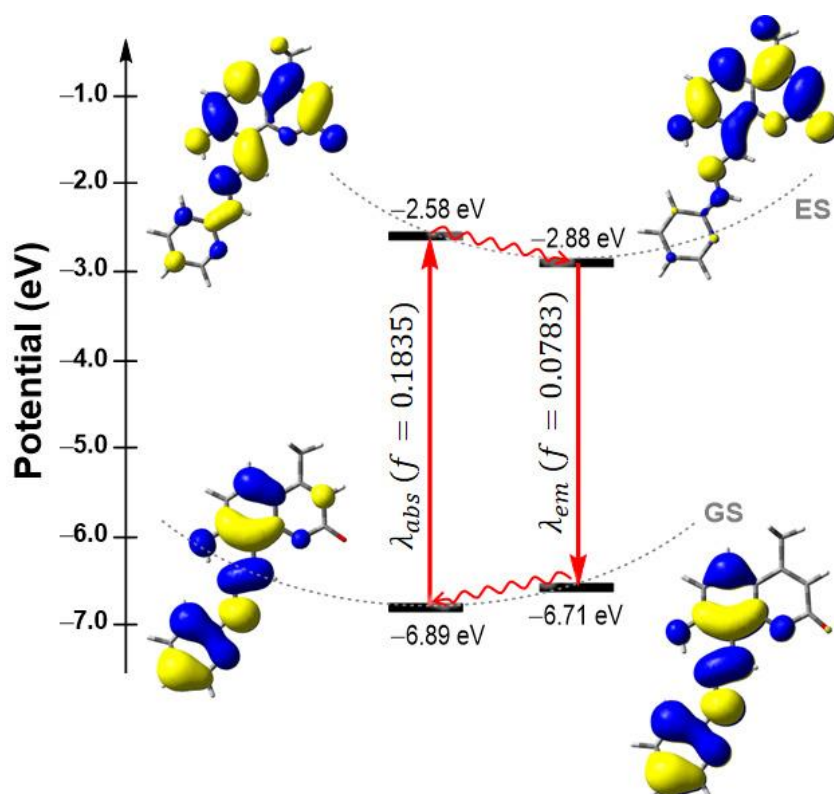


Figure S10. The frontier molecular orbitals and their relative energy levels of CMR-*o*-Py in the ground and excited states. GS: ground state. ES: excited state.

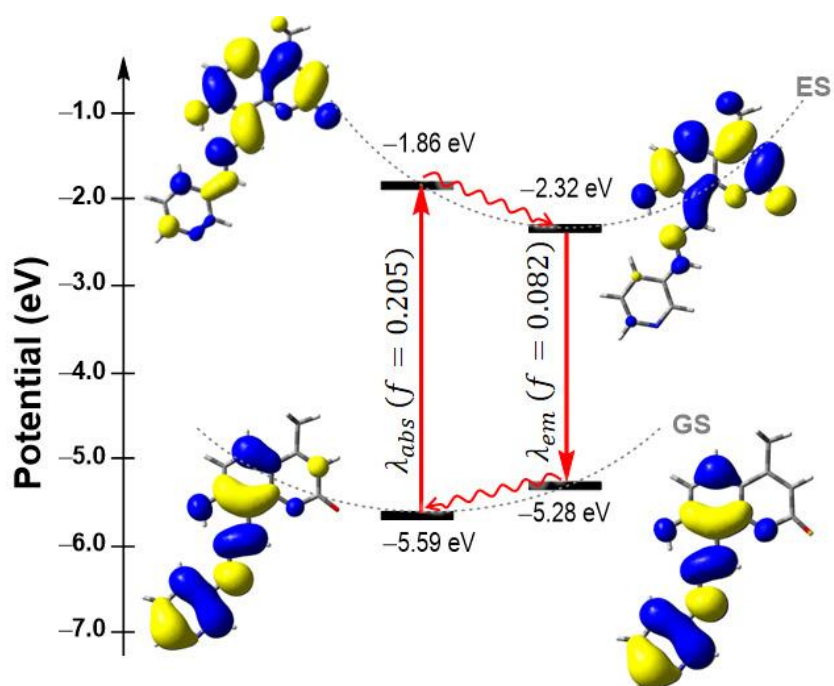


Figure S11. The frontier molecular orbitals and their relative energy levels of CMR-*m*-Py in the ground and excited states. GS: ground state. ES: excited state.

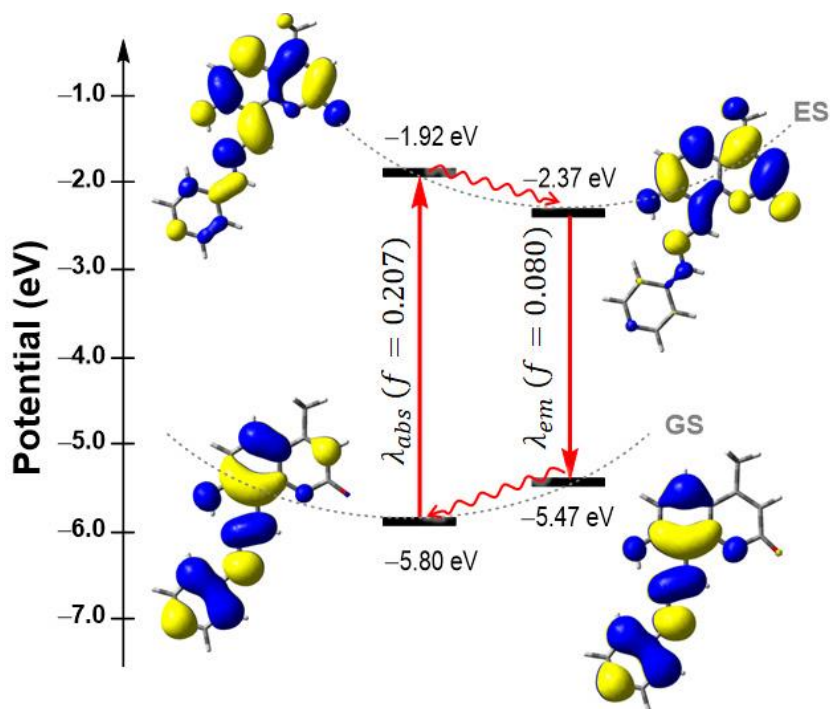


Figure S12. The frontier molecular orbitals and their relative energy levels of CMR-*p*-Py in the ground and excited states. GS: ground state. ES: excited state.

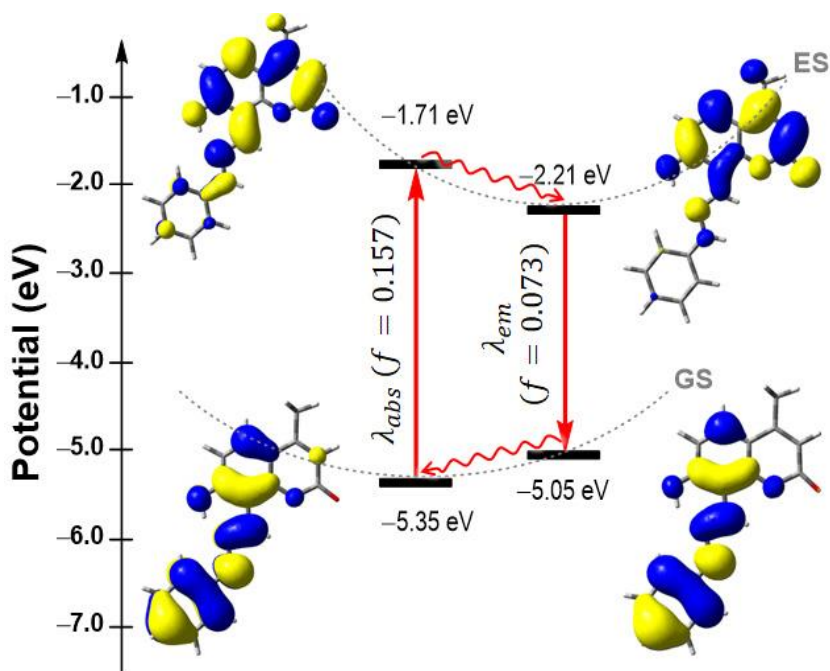


Figure S13. The frontier molecular orbitals and their relative energy levels of CMR-Ph in the ground and excited states. GS: ground state. ES: excited state.

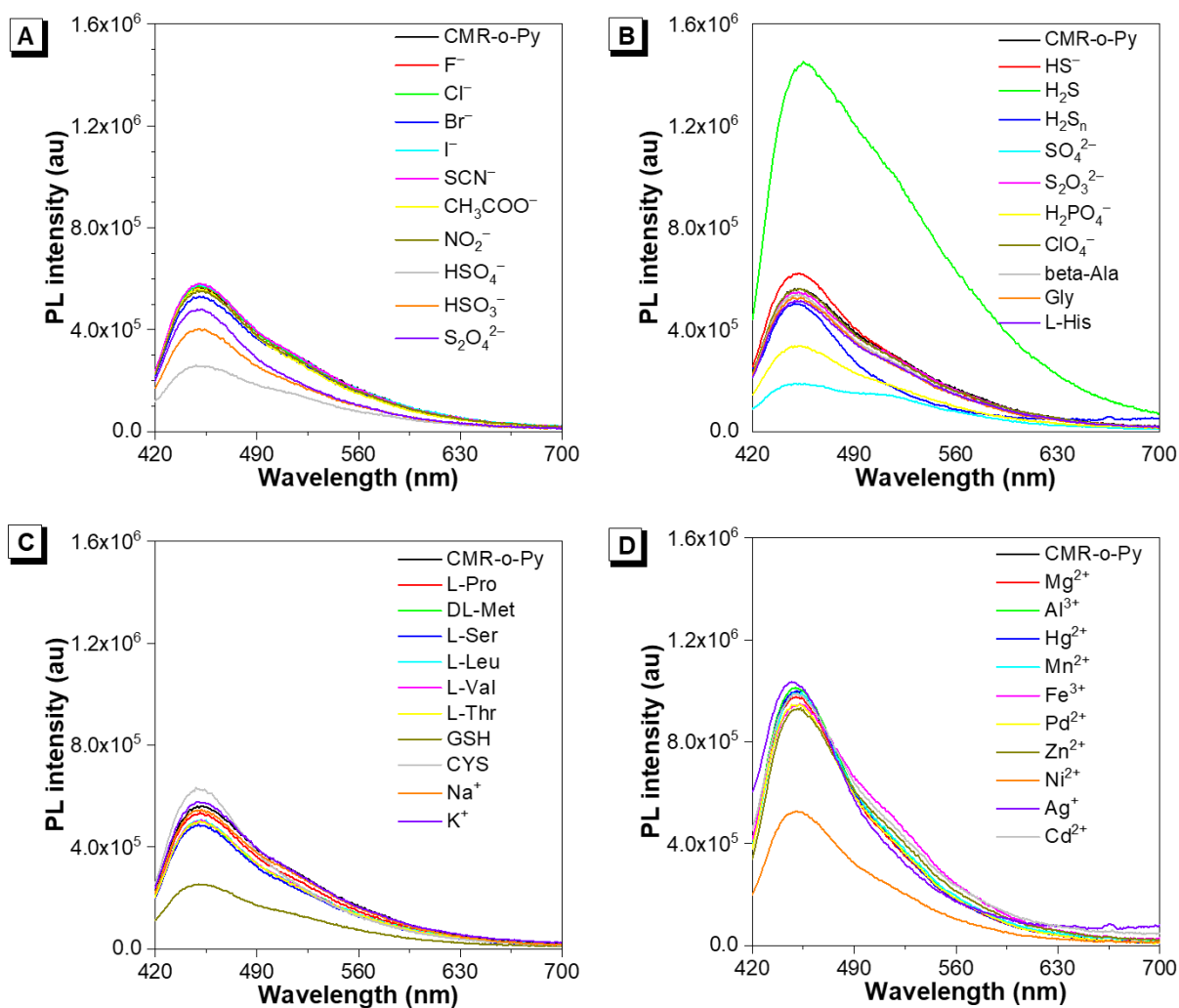


Figure S14. PL spectra of CMR-*o*-Py nanoaggregates in DMSO/PBS (1/9, v/v; pH = 7.4) mixture solutions (100 μ M) with different sulfide substances, amino acids, anions, and metal ions (1 mM). Excitation wavelength: 405 nm; excitation slit: 1 nm; emission slit: 5 nm.

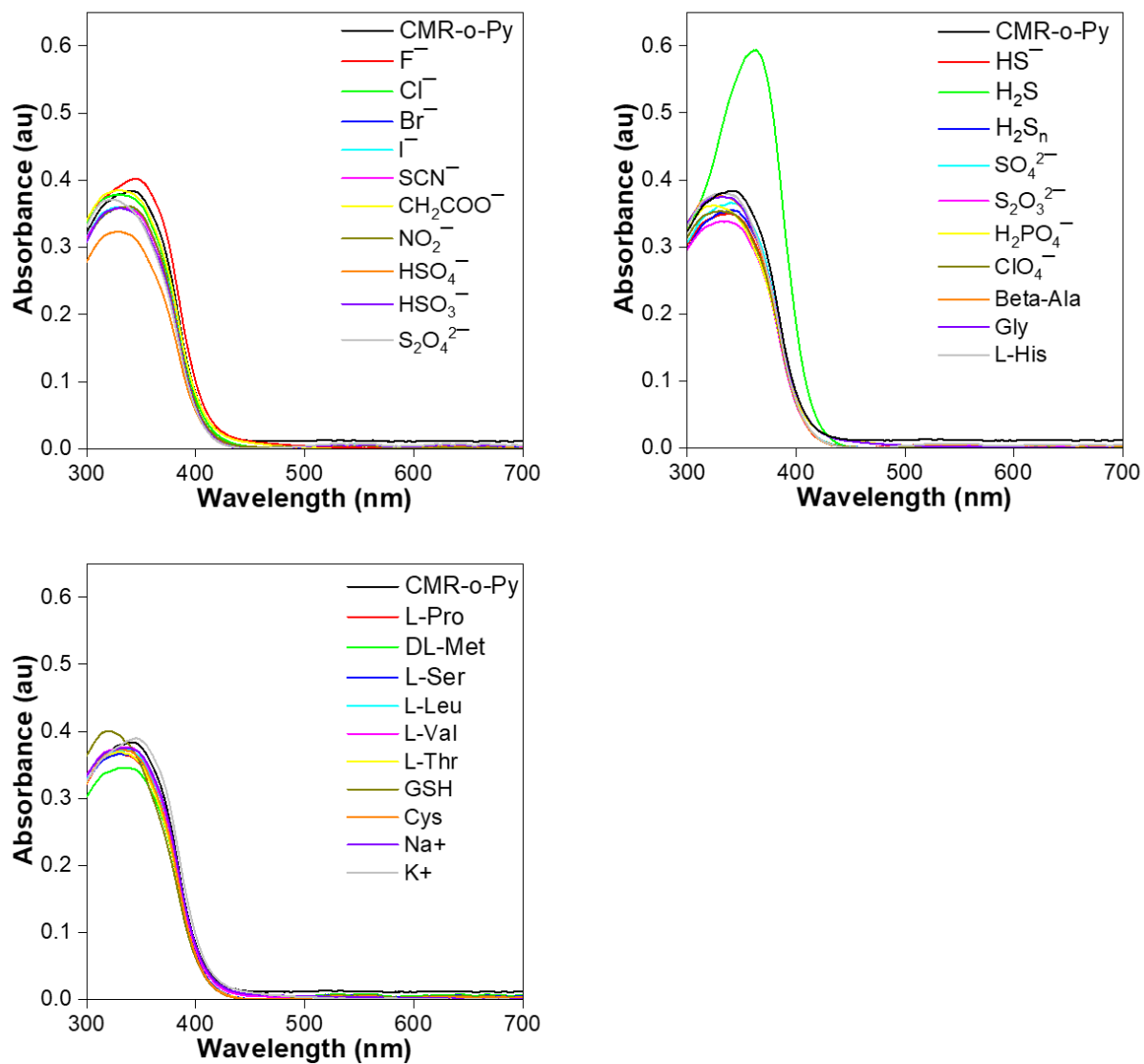


Figure S15. UV-vis absorption spectra of CMR-*o*-Py nanoaggregates in DMSO/PBS (1/9, v/v; pH = 7.4) mixture solutions (100 μM) with different sulfide substances.

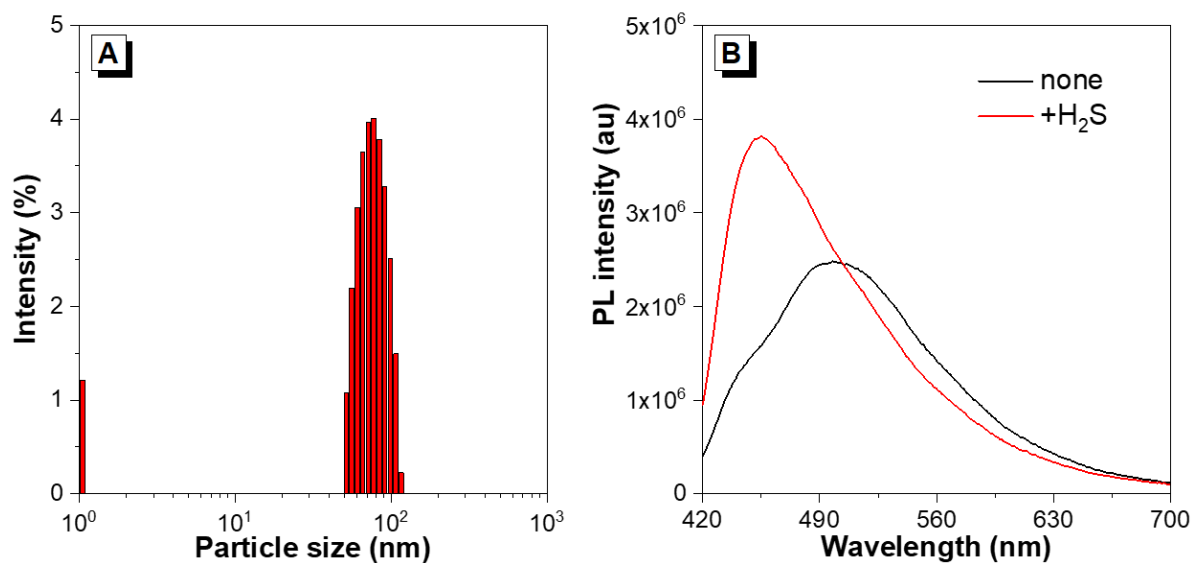


Figure S16. (A) DLS analysis of CMR-*o*-Py nanoaggregates in DMSO/PBS (4/6, v/v; pH = 7.4) mixture solutions (100 μ M) and (B) their PL spectra without and with H₂S (1 mM).

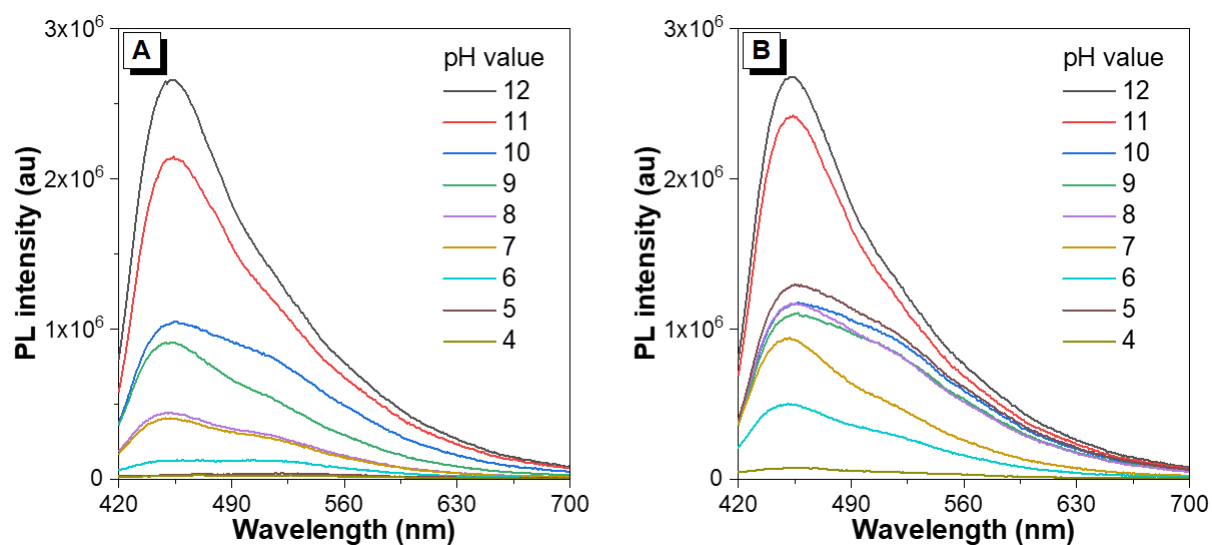


Figure S17. PL spectra of CMR-*o*-Py nanoaggregates (100 μ M in DMSO/PBS, 1/9, v/v; pH = 7.4) in different pH values (A) without and (B) with H₂S (1 mM). Excitation wavelength: 405 nm; excitation slit: 1 nm; emission slit: 5 nm.

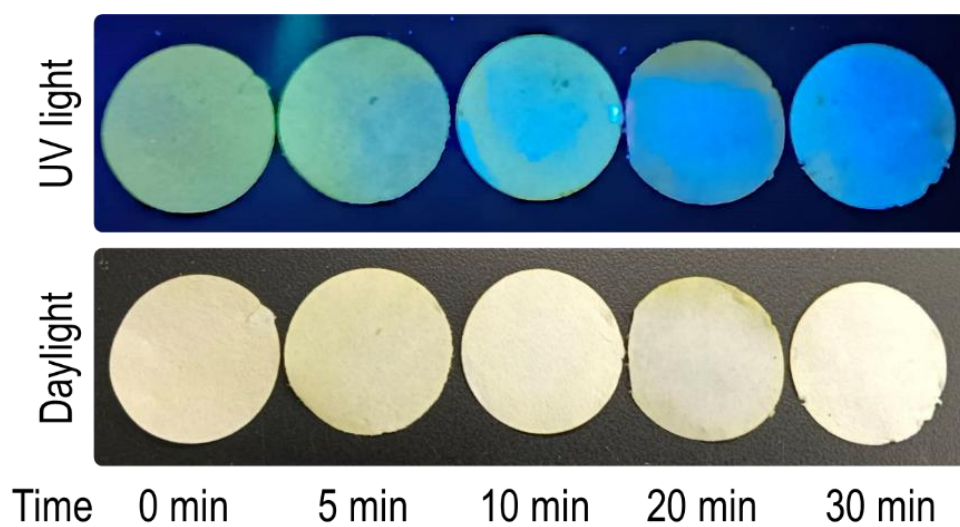


Figure S18. Photographs of CMR-*o*-Py nanoaggregates-adsorbed filter papers sensing H₂S gas during different times.

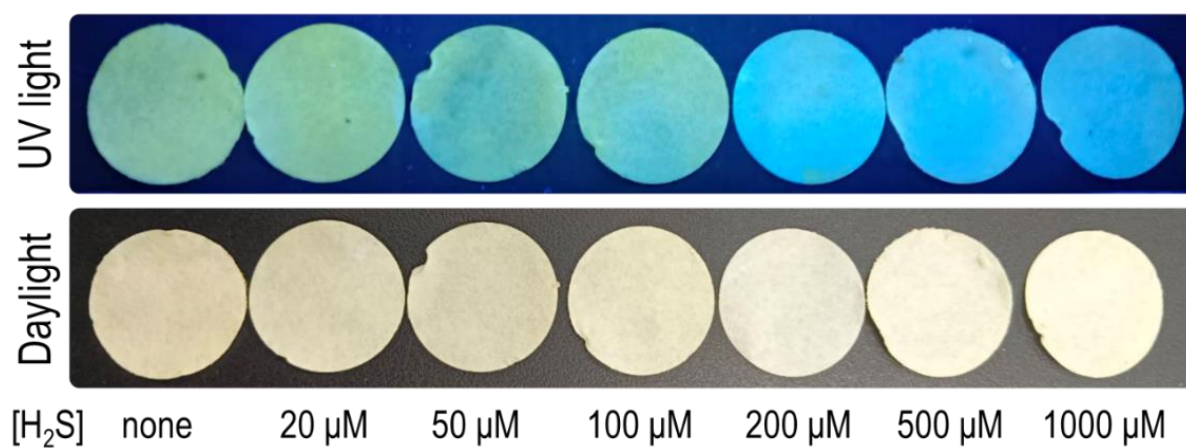


Figure S19. Photographs of CMR-*o*-Py nanoaggregates-adsorbed filter papers sensing different H₂S concentrations.

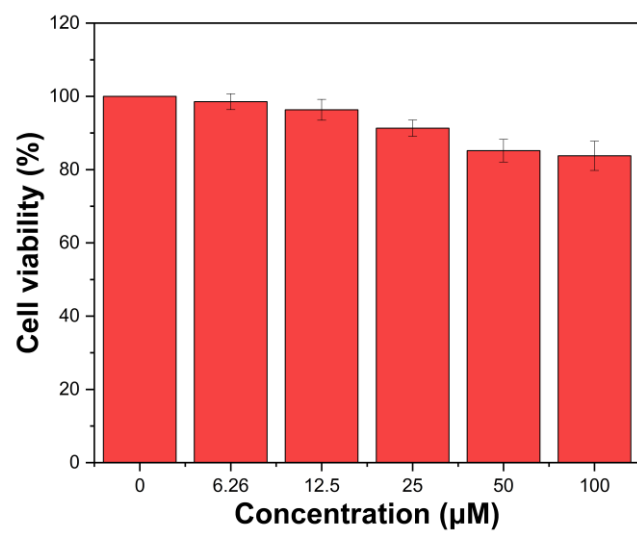


Figure S20. Cell viability of CMR-*o*-Py nanoaggregates with different concentrations.

Table S1. Calculation data of coumarin-based AIEgens in S_0 state.

Molecules	States	Configurations	E (eV)	λ (nm)	f_{os}
CMR-Ph	S_{01}	H-1 \rightarrow L (3%), H \rightarrow L (91%), H \rightarrow L+1 (5%)	3.26	379.78	0.16
	S_{02}	H-1 \rightarrow L (7%), H-1 \rightarrow L+1 (5%), H \rightarrow L (8%), H \rightarrow L+1 (79%)	3.68	337.32	0.52
	S_{03}	H-1 \rightarrow L (74%), H-1 \rightarrow L+1 (4%), H \rightarrow L+1 (14%), H \rightarrow L+3 (4%)	3.96	313.05	0.42
CMR- <i>o</i> -Py	S_{01}	H-1 \rightarrow L (7%), H \rightarrow L (85%), H \rightarrow L+1 (7%)	3.43	361.98	0.18
	S_{02}	H-1 \rightarrow L (22%), H-1 \rightarrow L+1 (7%), H \rightarrow L (13%), H \rightarrow L+1 (55%)	3.74	331.69	0.35
	S_{03}	H-1 \rightarrow L (59%), H \rightarrow L+1 (34%), H \rightarrow L+3 (3%)	3.99	310.49	0.65
CMR- <i>m</i> -Py	S_{01}	H-1 \rightarrow L (6%), H \rightarrow L (87%), H \rightarrow L+1 (6%)	3.38	367.02	0.20
	S_{02}	H-1 \rightarrow L (18%), H-1 \rightarrow L+1 (6%), H \rightarrow L (11%), H \rightarrow L+1 (63%)	3.69	335.91	0.38
	S_{03}	H-1 \rightarrow L (64%), H \rightarrow L+1 (27%), H \rightarrow L+3 (3%)	3.96	313.21	0.52
CMR- <i>p</i> -Py	S_{01}	H-1 \rightarrow L (12%), H \rightarrow L (78%), H \rightarrow L+1 (8%)	3.52	352.19	0.21
	S_{02}	H-1 \rightarrow L (31%), H-1 \rightarrow L+1 (6%), H \rightarrow L (20%), H \rightarrow L+1 (41%)	3.73	332.16	0.24
	S_{03}	H-1 \rightarrow L (48%), H \rightarrow L+1 (47%), H \rightarrow L+3 (2%)	4.02	308.56	0.72

* Calculated with TD-DFT at the level of B3LYP/6-31G*. S_{01} , S_{01} , and S_{03} denoted the first, second, and third vertical transition from the S_0 state to the S_1 , S_2 , and S_3 , respectively, and f_{os} denoted oscillator strength between the ground and excited states.

Table S2. Calculated data of coumarin-based AIEgens in S₁ state.

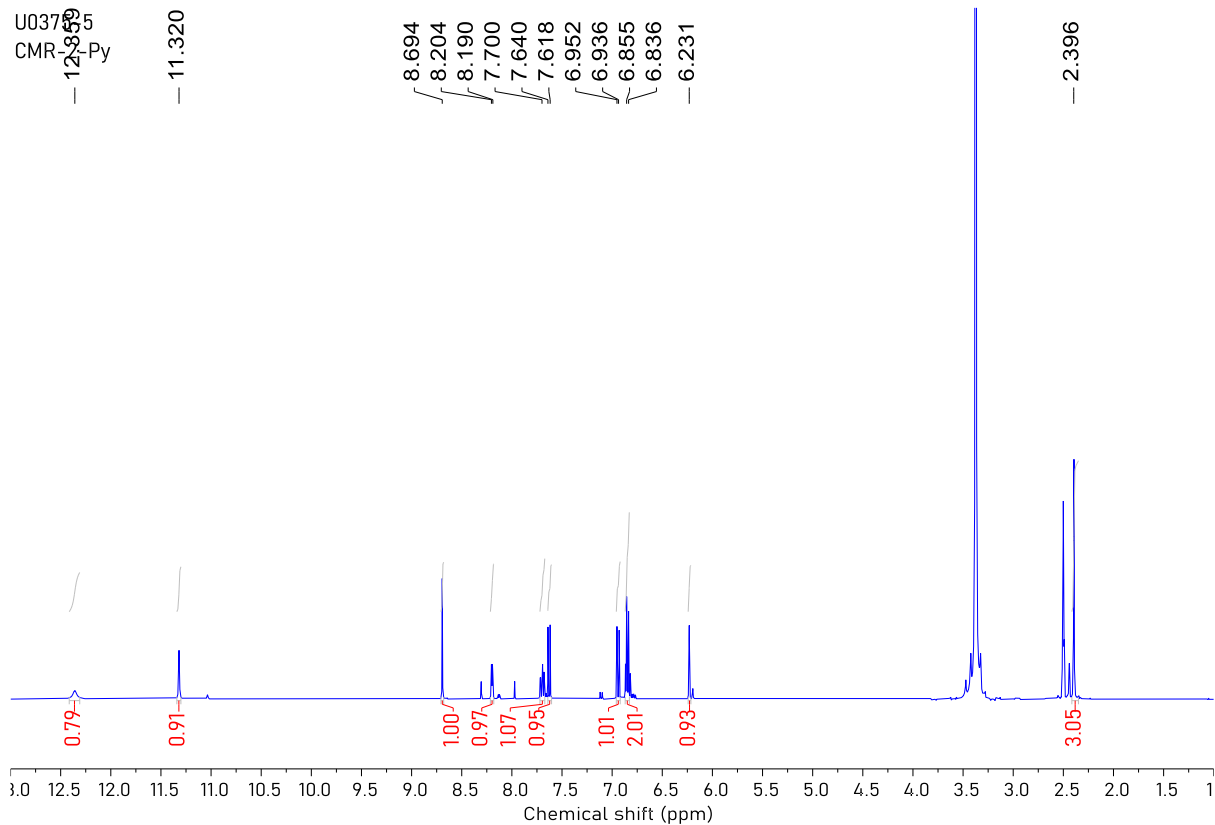
Molecules	Excited states	Configurations	<i>E</i> (eV)	λ (nm)	<i>f</i> _{os}
CMR-Ph	S ₁₀	H → L (98%)	2.44	507.84	0.07
CMR- <i>o</i> -Py	S ₁₀	H → L (96%), H → L+1 (2%)	2.60	476.07	0.08
CMR- <i>m</i> -Py	S ₁₀	H → L (97%)	2.56	483.92	0.08
CMR- <i>p</i> -Py	S ₁₀	H → L (96%), H → L+1 (2%)	2.67	464.37	0.08

* Calculated with TD-DFT at the level of B3LYP/6-31G*. S₁₀ denoted the first vertical radiation from the S₁ state to the S₀ state, and *f*_{os} denoted oscillator strength between the ground and excited states.

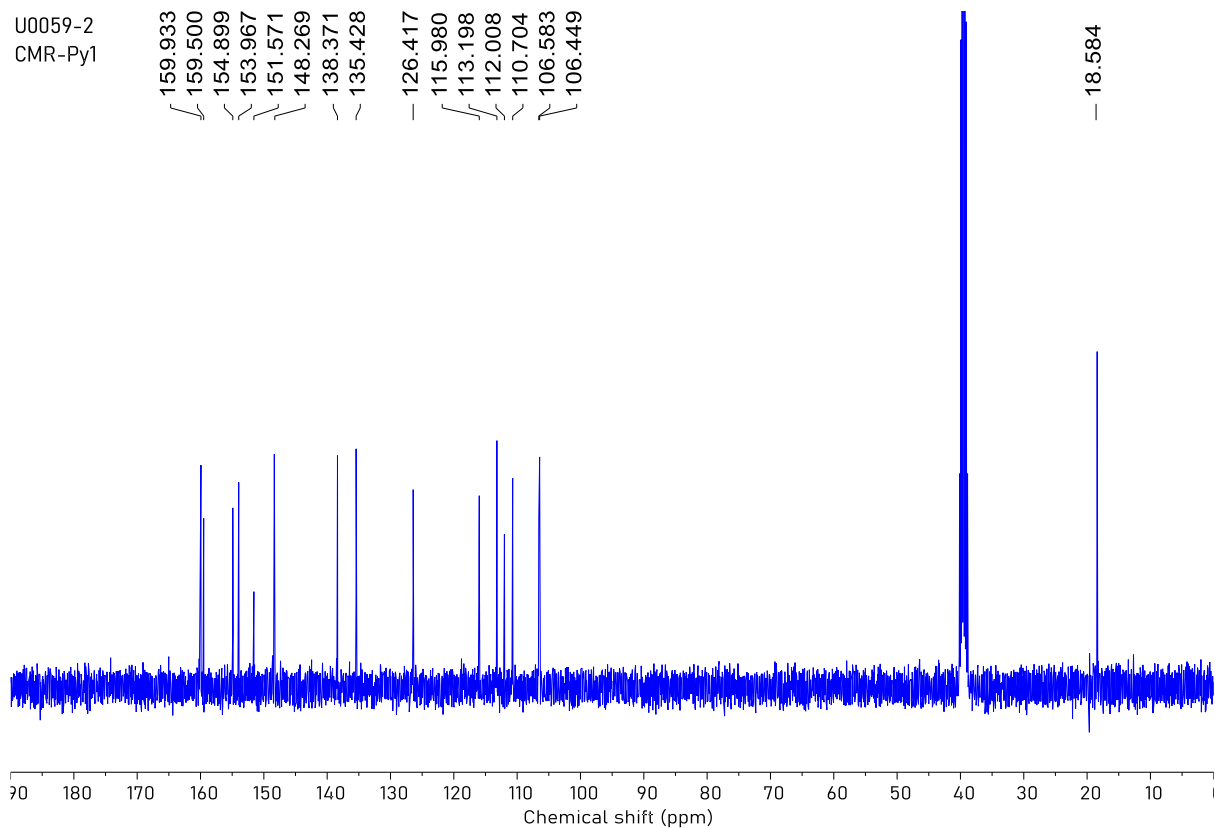
Table S3. Molecular dipole moments of coumarin-based AIEgens in S₀ and S₁ states.

Molecules	States	X (Debye)	Y (Debye)	Z (Debye)	Total (Debye)
CMR-Ph	S ₀	-0.1818	-2.0241	-0.0433	2.0327
	S ₁	-0.1818	-2.0241	-0.0433	2.0327
CMR- <i>o</i> -Py	S ₀	-0.1226	-3.8467	0.0002	3.8487
	S ₁	-5.5749	-1.5321	-0.0001	5.7816
CMR- <i>m</i> -Py	S ₀	-2.3291	-3.6224	0.0001	4.3066
	S ₁	-4.4721	-3.5658	0	5.7197
CMR- <i>p</i> -Py	S ₀	-3.5393	-1.5697	0.0001	3.8717
	S ₁	-2.104	-3.59	0	4.1611

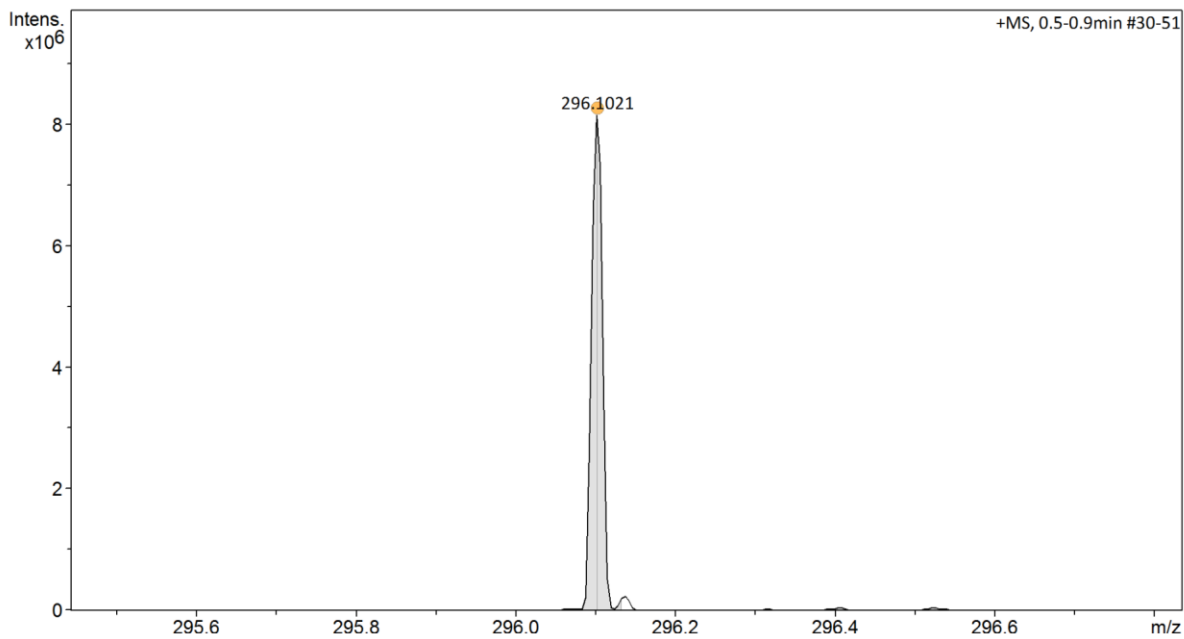
* Calculated with TD-DFT as the level of B3LYP/6-31G*.



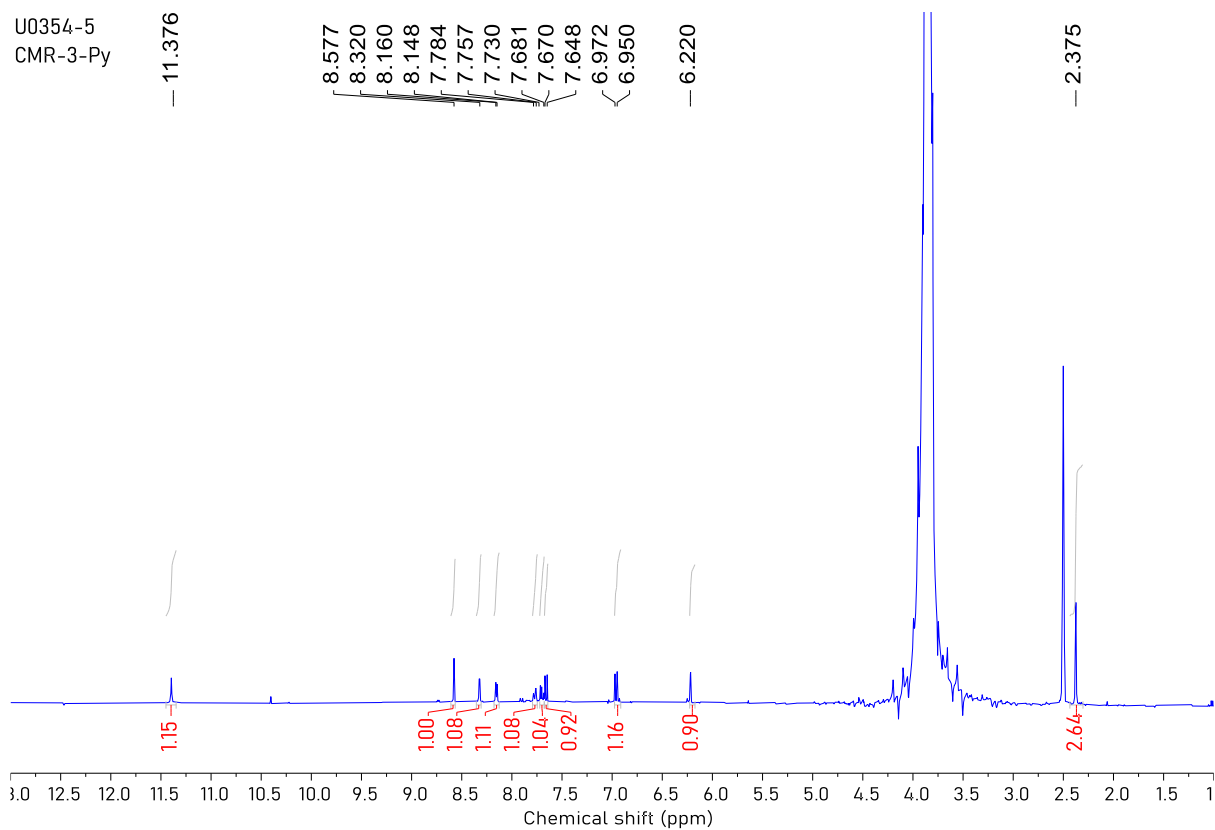
¹H NMR spectrum of CMR-*o*-Py.



¹³C NMR spectrum of CMR-*o*-Py.

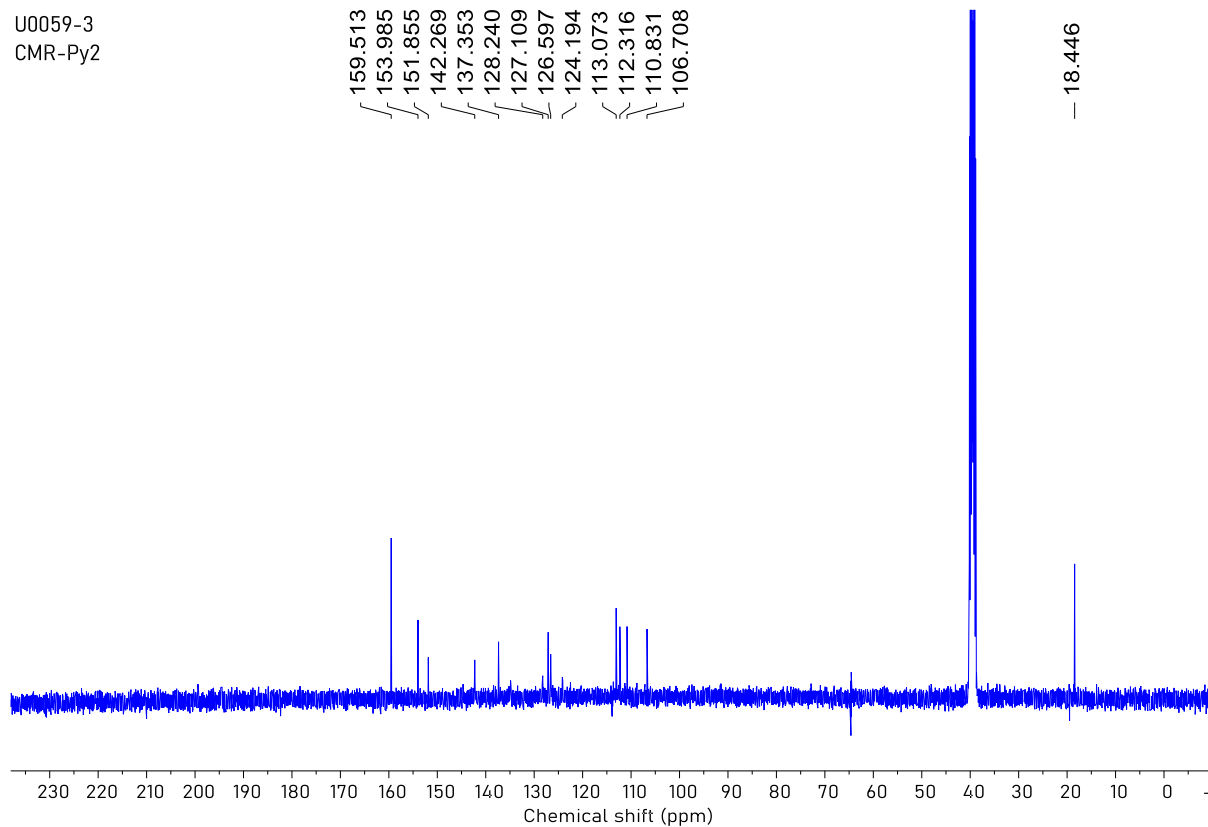


HRMS spectrum of CMR-*o*-Py.

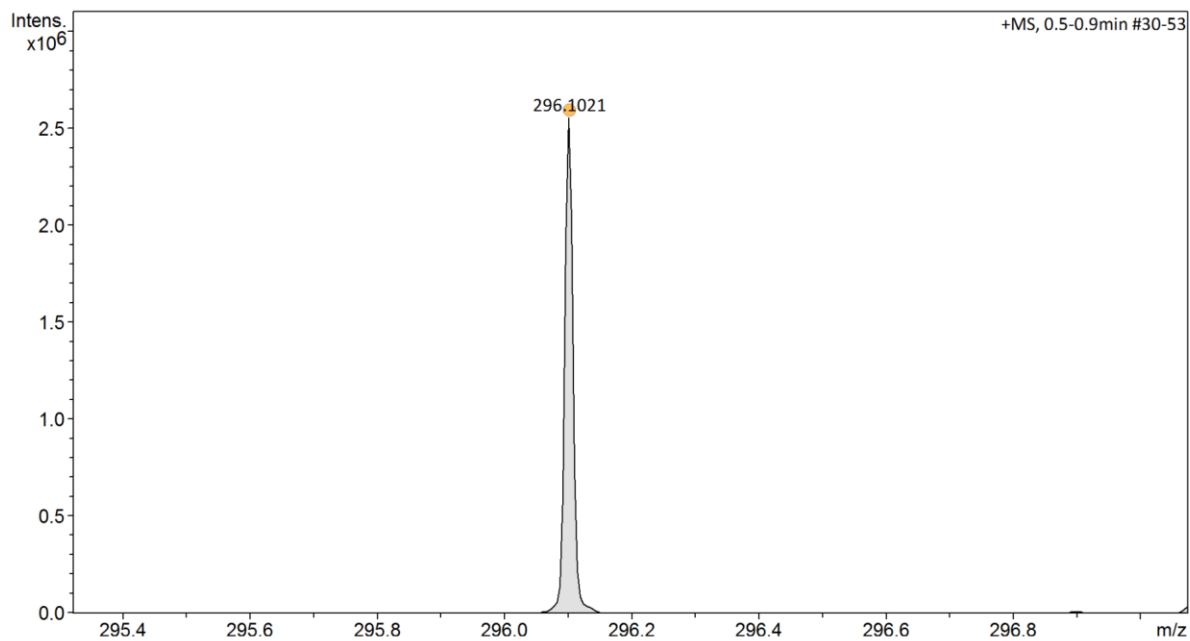


¹H NMR spectrum of CMR-*m*-Py.

U0059-3
CMR-Py2

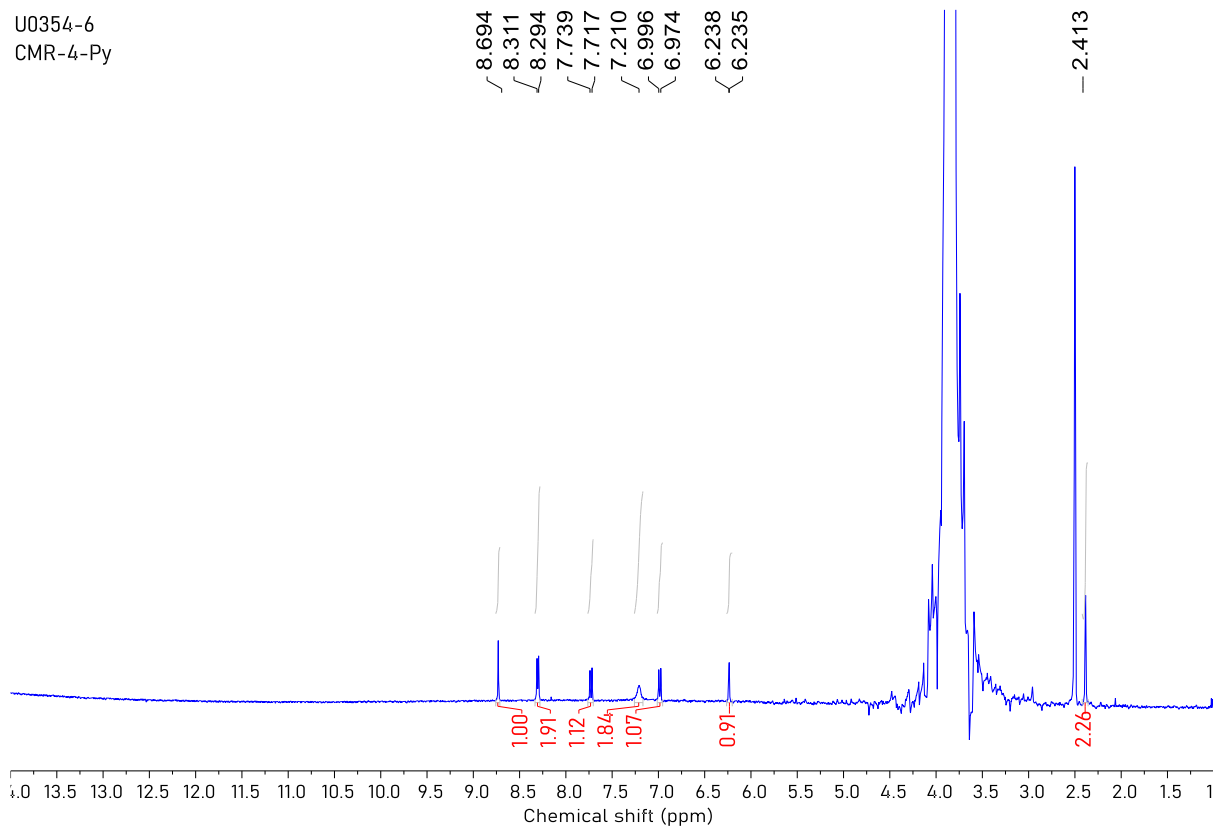


^{13}C NMR spectrum of CMR-*m*-Py.



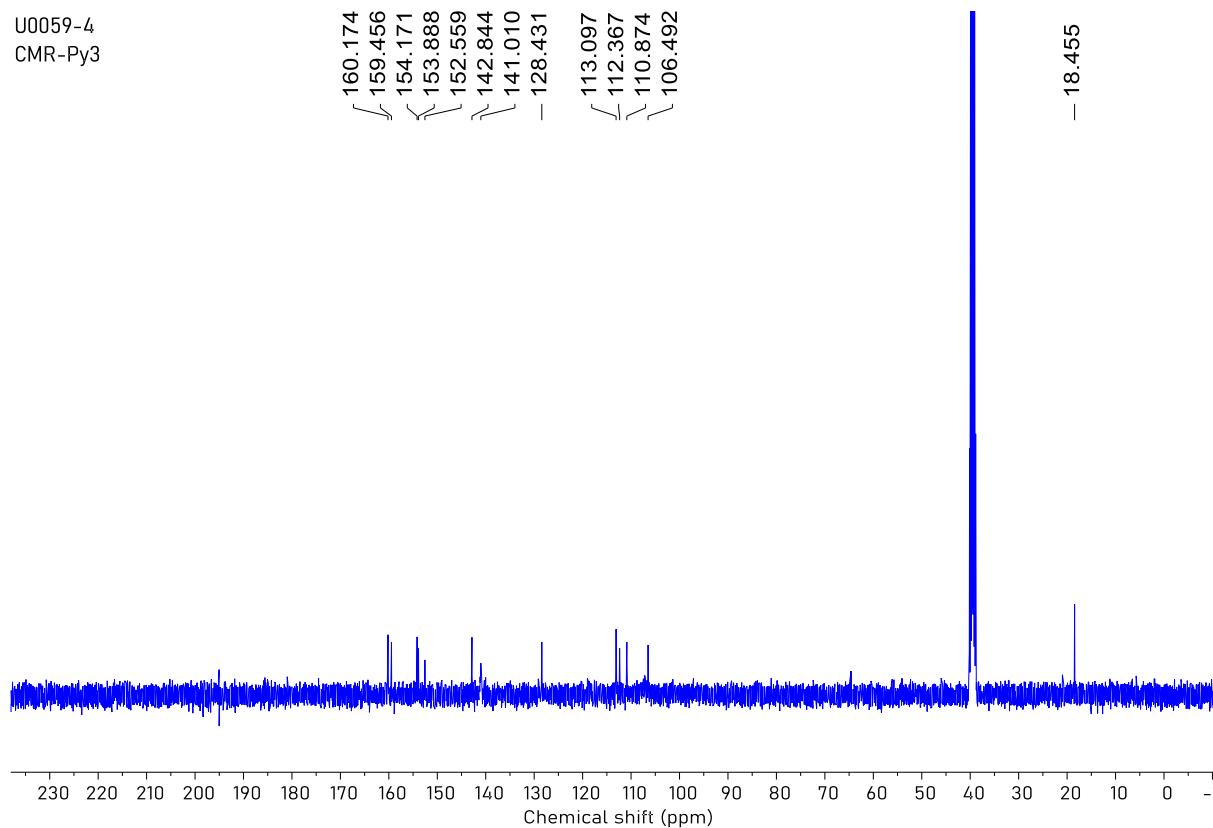
HRMS spectrum of CMR-*m*-Py.

U0354-6
CMR-4-Py

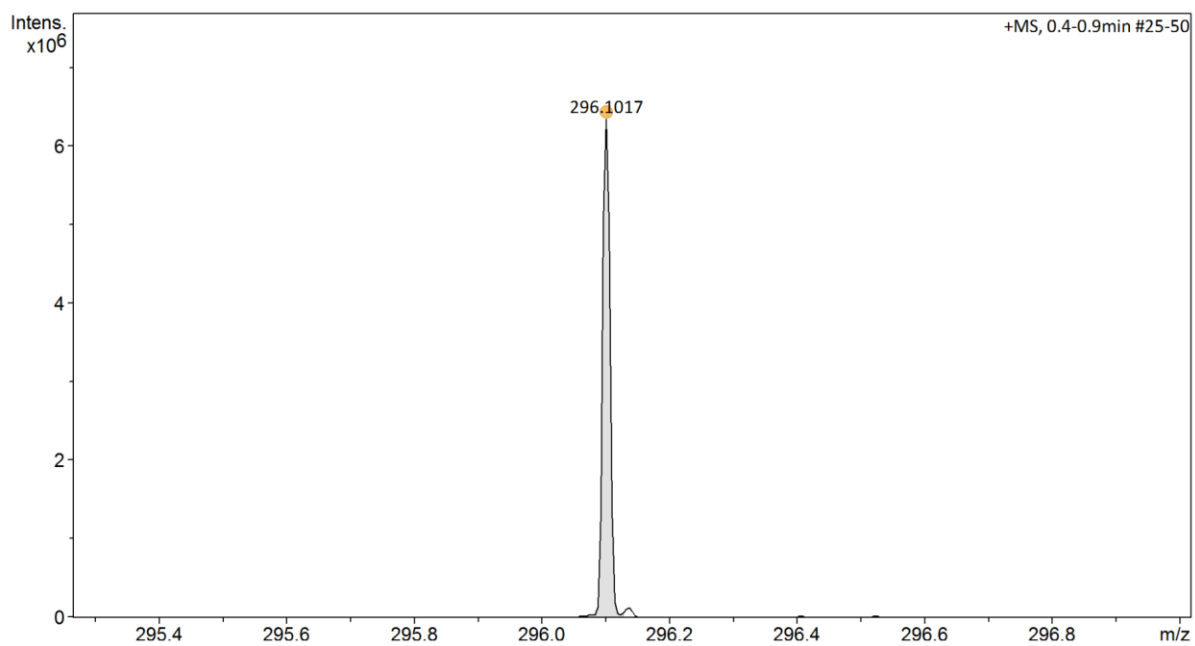


¹H NMR spectrum of CMR-*p*-Py.

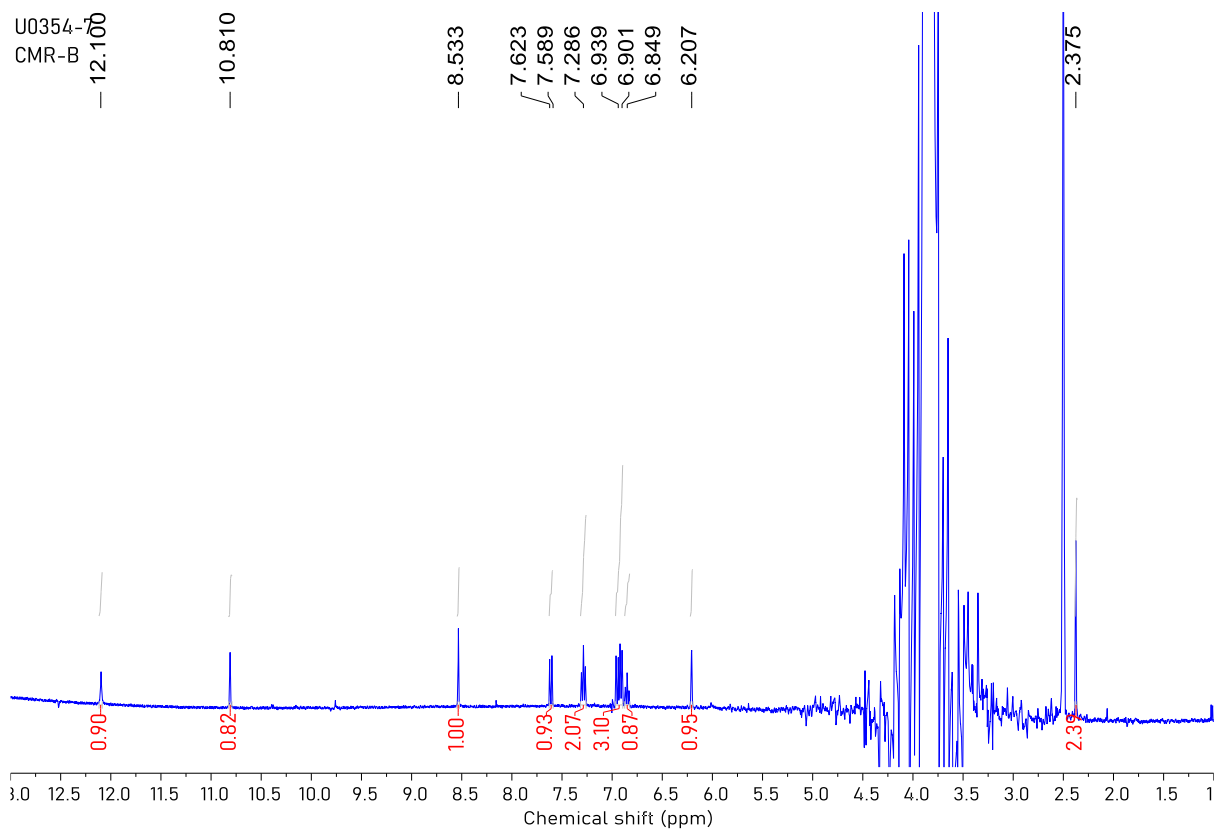
U0059-4
CMR-Py3



¹³C NMR spectrum of CMR-*p*-Py.

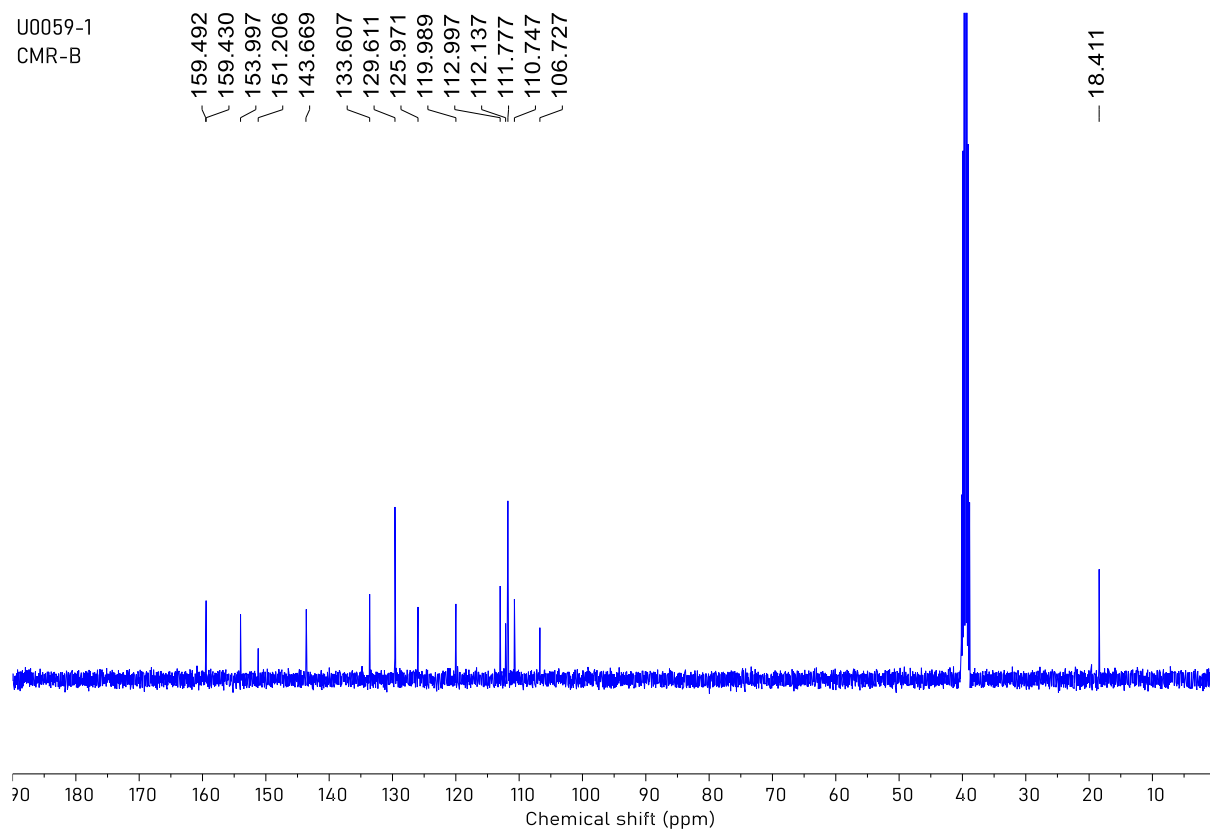


HRMS spectrum of CMR-*p*-Py.

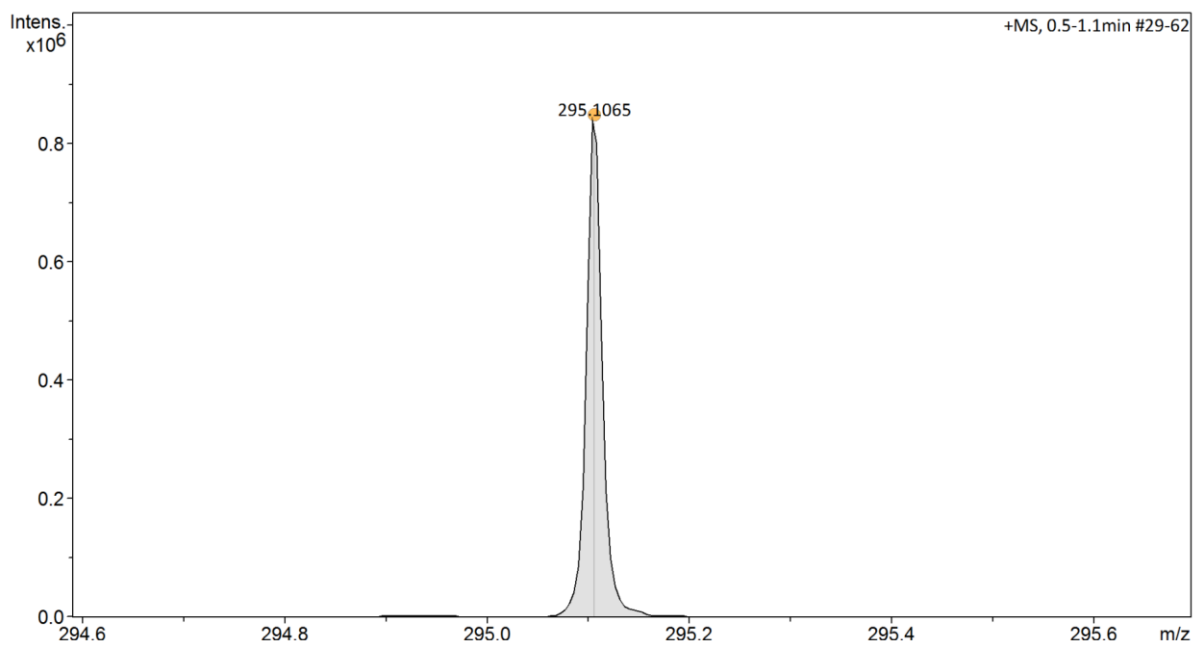


¹H NMR spectrum of CMR-Ph.

U0059-1
CMR-B



^{13}C NMR spectrum of CMR-Ph.



HRMS spectrum of CMR-Ph.